1-15-2012

Optimization of power and efficiency of thermoelectric devices with asymmetric thermal contacts

Kazuaki Yazawa
Birck Nanotechnology Center, Purdue University; University of California Santa Cruz, kyazawa@purdue.edu

Ali Shakouri
Birck Nanotechnology Center, Purdue University; University of California Santa Cruz, shakouri@purdue.edu

Yazawa, Kazuaki and Shakouri, Ali, "Optimization of power and efficiency of thermoelectric devices with asymmetric thermal contacts" (2012). *Birck and NCN Publications.* Paper 1263.
http://dx.doi.org/10.1063/1.3679544

AIP | Journal of Applied Physics

Optimization of power and efficiency of thermoelectric devices with asymmetric thermal contacts

Kazuaki Yazawa and Ali Shakouri

Citation: J. Appl. Phys. **111**, 024509 (2012); doi: 10.1063/1.3679544
View online: http://dx.doi.org/10.1063/1.3679544
View Table of Contents: http://jap.aip.org/resource/1/JAPIAU/v111/i2
Published by the AIP Publishing LLC.

Optimization of power and efficiency of thermoelectric devices with asymmetric thermal contacts

Kazuaki Yazawa[1,a)] and Ali Shakouri[1,2]
[1]*Baskin School of Engineering, University of California Santa Cruz, Santa Cruz, California 95064, USA*
[2]*Birck Nanotechnology Center, Purdue University, West Lafayette, Indiana 47907, USA*

(Received 22 September 2011; accepted 20 December 2011; published online 26 January 2012)

We report the theoretical efficiency of thermoelectric power generation with asymmetric thermal contacts to reservoirs. A key ingredient is the electrical and thermal co-optimization. Generic formula of the maximum power output and the optimum leg length are obtained. The Curzon-Ahlborn limit at maximum power can be rigorously derived when the dimensionless figure-of-merit is very large for any asymmetric thermal contact resistances. The results differ from cyclic thermodynamic engines, and some of the reasons are discussed. We also point out the similarity and differences with single-level quantum dot heat engines, which assume no explicit thermal contact resistance with reservoirs. © *2012 American Institute of Physics*. [doi:10.1063/1.3679544]

I. INTRODUCTION

Research efforts on thermoelectrics have been mostly focused on improving the dimensionless figure-of-merit (ZT) of the material.[1–3] Z is the ratio of the Seebeck coefficient square times electrical conductivity divided by thermal conductivity, and T is the absolute temperature. Improving the material ZT (with, e.g., embedded nanoparticles, superlattice, etc.) is not the only factor which affects the power output. We need to consider the whole energy conversion system, which involves thermal contacts with the hot and cold reservoirs. Recently, it was shown that the system efficiency at maximum power output is inversely proportional to the sum of the heat dissipation in hot and cold thermal resistances.[4] The optimum condition is found only when the thermoelectric internal impedance matches the external impedance both electrically and thermally. This fact has been partially understood and reported in the literature on thermoelectric systems.[5–9] Here, we perform a comprehensive optimization by the method of the Lagrange multiplier based on a generic model of a thermoelectric generator with asymmetric thermal contacts with reservoirs. We use this model to identify the efficiency at large ZT and compare the results with ideal thermodynamic engines. We also discuss the differences compared to single level quantum dot thermoelectric heat engines.

II. MODEL

The model includes a thermoelectric element (leg) with length d placed between hot and cold reservoirs. The thermal resistance with the hot reservoir is given by ψ_h, and that with the cold reservoir is ψ_c, as shown in Fig. 1. This model considers a unit cross-sectional area, which is perpendicular to the heat flow. Heat flux q_h is supplied by the hot reservoir at temperature T_s (fixed). Also, the cold reservoir T_a (fixed) is given. Heat flux q_c, which flows into the cold reservoir, is reduced from q_h, depending on the energy conversion efficiency. Useful power w is extracted at the external electrical load resistor R_L connected to the leg.

For a given material system (with any Z value), the system could be designed to operate either at maximum output power or at maximum efficiency. The system parameters that can be changed are: external thermal resistances with hot and cold reservoirs, thermoelectric (TE) element thickness, and load resistance. In practice, there is always some finite thermal resistance between the TE element and reservoirs and this is given. Then, TE element thickness and load resistance are variables that should be adjusted to be able to get the highest output power or the highest efficiency. The difficulty is that changing the thermoelectric leg length affects temperatures at the hot and cold sides of the element, which, in turn, modify Peltier cooling and heating at interfaces. The equations become recursive and a careful co-optimization of the electrical and thermal networks is required. This is a mathematical difficulty, which is described in Sec. III. However, from a physical point of view, the picture is clear. The highest output power corresponds to the highest power delivered to a load. The highest efficiency corresponds to the highest ratio of electrical power delivered to load to the amount of heat flux from the hot reservoir to the cold reservoir.

Equations (1) and (2) are derived based on the energy conservation at two nodes, T_h and T_c, which are the temperatures at the hot side and the cold side of the thermoelectric leg.

$$q_h = \frac{\beta}{d}(T_h - T_c) + SIT_h - I^2R/2, \tag{1}$$

$$q_c = \frac{\beta}{d}(T_h - T_c) + SIT_c + I^2R/2. \tag{2}$$

Here, β is the thermal conductivity, S is the Seebeck coefficient, I is the electrical current, and R is the thermoelectric internal (electrical) resistance. One should note that Joule heating happens everywhere in the thermoelectric leg. In one-dimensional heat transport, one can show that Joule heating could be represented by two localized sources at the hot and the cold junctions, each dissipating $1/2$ of the total

a)Author to whom correspondence should be addressed. Electronic mail: kaz@soe.ucsc.edu.

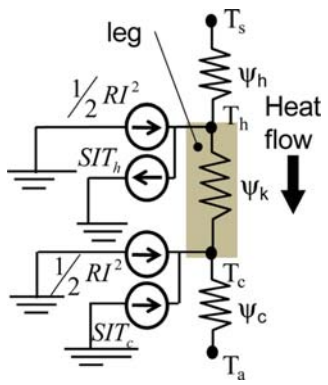

FIG. 1. (Color online) Thermal resistance network showing a thermoelectric leg in contact with hot and cold reservoirs. Peltier and Joule heating sources are also shown.

power. The output power delivered to the load per unit area of the heat source w [W/m^2] is found as

$$w = I^2 mR = \frac{m\sigma S^2}{(1+m)^2 d}(T_h - T_c)^2, \tag{3}$$

where $w = q_h - q_c$ by energy conservation, σ is electrical conductivity of the leg, and m is the ratio of the internal resistance to the external load resistance, i.e., $R_L = mR$. The ratio of the temperature difference across thermoelectric leg $(T_h - T_c)$ over the overall temperature difference $(T_s - T_a)$ can be calculated from the energy balance equation as

$$\frac{(T_h - T_c)}{(T_s - T_a)} = \frac{d}{d + \beta(X+Y)}, \tag{4}$$

where X and Y are

$$X = \left(1 + \frac{Z}{2(1+m)^2}((2m+1)T_h + T_c)\right)\psi_h,$$
$$Y = \left(1 + \frac{Z}{2(1+m)^2}(T_h + (2m+1)T_c)\right)\psi_c, \tag{5}$$

where Z is the figure of merit. Thus, the power output as a function of T_s and T_a can be written as

$$w = \frac{mZ}{(1+m)^2}\frac{d\beta}{\left(d + \beta(X+Y)\right)^2}(T_s - T_a)^2. \tag{6}$$

The temperatures T_h and T_c in Eq. (5) can be found using recursive Eqs. (7) and (8) below, which are transformed from the energy balance Eqs. (1) and (2). In subsequent analysis and numerical tests, these T_h and T_c are calculated iteratively.

$$g_1 = \frac{\beta}{d}X(T_h - T_c) - (T_s - T_h) = 0, \tag{7}$$

$$g_2 = \frac{\beta}{d}Y(T_h - T_c) - (T_c - T_a) = 0. \tag{8}$$

III. OPTIMIZATION FOR MAX POWER OUTPUT

We maximize the power output, which depends on several parameters m, d, T_h, and T_c. The Lagrange multiplier method was used for the optimization. Taking partial derivatives of Eq. (6) with respect to m, d, T_h, and T_c, while introducing constraint functions Eqs. (7) and (8), we obtain the following eight equations:

$$\frac{\partial w}{\partial m} - \lambda_1\frac{\partial g_1}{\partial m} = 0,\ \frac{\partial w}{\partial d} - \lambda_1\frac{\partial g_1}{\partial d} = 0,\ \frac{\partial w}{\partial T_h} - \lambda_1\frac{\partial g_1}{\partial T_h} = 0,$$
$$\frac{\partial w}{\partial T_c} - \lambda_1\frac{\partial g_1}{\partial T_c} = 0, \frac{\partial w}{\partial m} - \lambda_2\frac{\partial g_2}{\partial m} = 0,\ \frac{\partial w}{\partial d} - \lambda_2\frac{\partial g_2}{\partial d} = 0,$$
$$\frac{\partial w}{\partial T_h} - \lambda_2\frac{\partial g_2}{\partial T_h} = 0,\ \frac{\partial w}{\partial T_c} - \lambda_2\frac{\partial g_2}{\partial T_c} = 0. \tag{9}$$

We first find the Lagrange multiplier λ_1 and λ_2 from the two above Lagrange differentials of w with m as

$$\lambda_1 = \frac{(m-1)(T_h - T_c)}{\psi_h(mT_h + T_c)},\quad \lambda_2 = \frac{(m-1)(T_h - T_c)}{\psi_c(T_h + mT_c)}. \tag{10}$$

Then, we find the optimum m (e.g., m_{opt}) by substituting Eq. (10) into λ_1 and λ_2 in the two above Lagrange differentials of w with respect to d. These two equations yield the same result as

$$m_{opt} = \sqrt{1 + Z\frac{(T_h + T_c)}{2}}. \tag{11}$$

Note that this m is still not independent from T_h and T_c. From the rest of the Lagrange differentials of w, with respect to T_h and T_c, the leg length d is found for maximum power output as

$$\frac{d_h}{\beta} = \frac{\psi_h\left(T_h + (2m-1)T_c\right)}{(T_h + T_c)},\quad \frac{d_c}{\beta} = \frac{\psi_c\left((2m-1)T_h + T_c\right)}{(T_h + T_c)}. \tag{12}$$

Unfortunately, we did not reach a unique solution for optimum leg length. In Eq. (12), subscripts h and c denote the origin of the equations in the Lagrange differentials T_h and T_c, respectively. By our extensive numerical tests, we were able to eventually obtain the solution of the optimum leg length as the sum of the two equations in Eq. (12),

$$\frac{d_{opt}}{\beta} = \frac{\psi_h\left(T_h + (2m-1)T_c\right) + \psi_c\left((2m-1)T_h + T_c\right)}{(T_h + T_c)}. \tag{13}$$

For the symmetric contacts $\psi_h = \psi_c$, the optimum leg length becomes quite simple as

$$\frac{d_{opt}}{\beta} = m\sum\psi. \tag{14}$$

Here, $\Sigma\psi$ is the sum of the external thermal resistances, i.e., $\Sigma\psi = \psi_h + \psi_c$. The m in the above Eqs. (13) and (14) must simultaneously obey Eq. (11) to calculate the optimum leg length.

Then, two temperatures T_h and T_c at the maximum power output are found from the given temperatures T_s and T_a. The ratio $\alpha = (T_s - T_a)/(T_h - T_c)$ is found from Eqs. (4) and (13) as

$$\alpha = \frac{(2m-1)(m+1)(\psi_h+\psi_c)(T_h+T_c) + 2\left(\psi_h(T_h+mT_c)+\psi_c(mT_h+T_c)\right)}{(m+1)\left(\psi_h\left(T_h+(2m-1)T_c\right)+\psi_c\left((2m-1)T_h+T_c\right)\right)}. \tag{15}$$

The temperature difference across the leg is half of the total temperature difference at the maximum power output according to Eq. (15) only if $\psi_c/\psi_h = 1$.

$$\alpha_{symmetry} = \frac{T_s - T_a}{T_h - T_c} = 2. \tag{16}$$

From this analysis, the maximum power output shall be found near the point at which the internal and external temperature differences match, analogous to the voltage difference match in an electronic circuit. Due to the thermoelectric energy conversion, the thermal resistance match takes into account the reduction of effective thermal conductance of the leg due to the power generation.

From Eqs. (6) and (7), the relation of temperature ratio T_a/T_s and T_c/T_h is found as

$$\frac{T_a}{T_s} = \frac{\left(\psi_c\left(2m(T_h+mT_c)\right)+(m+1)\{\psi_h\left(T_h+(2m-1)T_c\right)+\psi_c\left((2m-1)T_h+T_c\right)\}\right)T_c - \psi_c\left(2m(T_h+mT_c)\right)T_h}{\left(\psi_h\left(2m(mT_h+T_c)\right)+(m+1)\{\psi_h\left(T_h+(2m-1)T_c\right)+\psi_c\left((2m-1)T_h+T_c\right)\}\right)T_h - \psi_h\left(2m(mT_h+T_c)\right)T_c}. \tag{17}$$

These temperatures T_c and T_h should be determined from the above Eqs. (15) and (17). However, the equations are still too complex to yield the closed forms. Finally, the maximum power output is found as

$$w_{\max} = \frac{mZ}{\alpha^2(1+m)^2}\frac{\beta}{d_{opt}}(T_s - T_a)^2. \tag{18}$$

Equation (18) is one of the key results of this paper, and it is valid for any value of Z. This equation is valid when the optimum thickness of the TE element for highest output power is given by Eq. (13) and the optimum value of load resistance with respect to TE leg resistance, m, is given by Eq. (11). In Eq. (18), m, d_{opt}, and α still depend on T_h and T_c. T_h and T_c can be derived from T_s and T_a using Eqs. (15) and (17). Equation (18) shows how maximum power output depends on asymmetric external thermal resistances ψ_c and ψ_h. For symmetric contact systems,

$$w_{\max} = \frac{Z}{4(1+m)^2\sum\psi}(T_s - T_a)^2. \tag{19}$$

This explains the result of Freunek *et al.*[9]. Their model gives the maximum without the term $(1+\mathrm{m})^2$, and thus, it is valid only if $\mathrm{m} \sim 1$.

IV. EFFICIENCY ANALYSIS

The energy conversion efficiency η at maximum power output is given by w_{max} divided by q_h. From the Eqs. (1), (11), and (18), the system efficiency becomes

$$\eta = \frac{(m-1)(T_h - T_c)}{(mT_h + T_c)}. \tag{20}$$

This equation is exactly the same as the well-known formula of the maximum efficiency of thermoelectric elements. T_h and T_c depend on the system boundary conditions, and they need to be derived as a function of T_s and T_a, iteratively, using Eqs. (15) and (17).

In the following, we assumed an infinitely large Z to find the upper limit of system efficiency at the maximum power output. Since the temperatures T_h and T_c have a weak dependence on ψ_c/ψ_h, the efficiency changes slightly. Interestingly, the efficiency converges to a unique formula as Z goes to infinity.

At Z → infinity, the Eq. (17) converges as

$$\frac{T_s}{T_a} \to \left(\frac{T_h}{T_c}\right)^2. \tag{21}$$

Therefore, the efficiency Eq. (20) at the maximum power output when Z → infinity is given by

$$\eta \to 1 - \frac{T_c}{T_h} = 1 - \sqrt{\frac{T_a}{T_s}}. \tag{22}$$

Eq. (22) is independent of either ψ_c or ψ_h. Thus, this efficiency applies to all asymmetric thermal contacts. This is exactly the same efficiency at the maximum power output for the irreversible thermodynamic engine, which was derived by Curzon and Ahlborn.[10]

Now, let us study the case when the leg length is fixed to the optimum value found for the symmetric thermal

resistances and then change the load resistance to get highest power in the case of asymmetric thermal resistances. The total $\psi_c + \psi_h$ is assumed to be constant. Figure 2(a) and 2(b) show that Curzon-Ahlborn efficiency at maximum power is found when the leg length is optimized for each asymmetric thermal resistance. Figure 2(b) also shows the efficiency if the leg length is kept constant (fixed d/β). In the latter case, the efficiency at the maximum power depends on the ψ_c/ψ_h ratio.

The optimization of output power for finite thermal resistances with heat source and heat sink is technologically important. As for any given heat source, we have a trade-off in the design of the thermoelectric generator and in the optimization of performance and cost of the high performance heat sinks (e.g., microchannel; see Ref. 12).

Figure 3 shows the higher bounds of the system efficiency at the maximum power output from the above cases when Z is very large. In the figure, Carnot efficiency is defined, as it should, as a function of reservoir temperatures $(1 - T_a/T_s)$. It is interesting to note that the asymmetric limits, when the optimum leg length is fixed to the value for the symmetric system, have very different behaviors for low hot-side thermal resistance or low cold-side thermal resistance. These limits are very similar to the ones for generic cyclic thermodynamic systems reported by Esposito *et al.*[11]. On the other hand, when the leg length is fully optimized, the thermoelectric generator recovers the Curzon-Ahlborn limit.

Figure 4(a) shows the power output as a function of relative efficiency with respect to the Carnot value when $T_a/T_s = 0.2$ as an example. The ZT parameter is modified by changing only the thermal conductivity. The leg length d is a variable along the curves. Curves start from zero and increase in both power output and efficiency as leg length d increases. After reaching a peak, power decreases, but efficiency continues to increase. This trend is observed for any ZT value. Only for the case of $ZT \rightarrow$ infinity does the maximum efficiency exactly match the Carnot efficiency, i.e.,

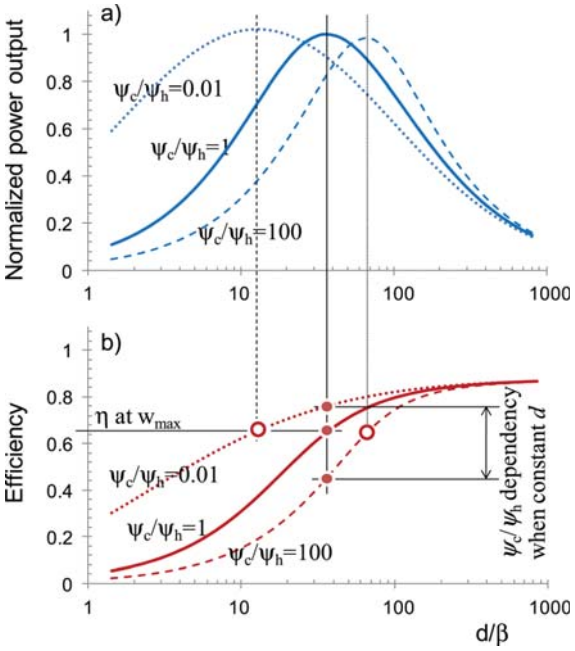

FIG. 2. (Color online) Power output normalized to the maximum at $\psi_c/\psi_h = 1$ and efficiency as a function of normalized leg length. $T_a/T_s = 0.1$, $Z = 1$ (order of ZT $\sim 10^3$), $\psi_c/\psi_h = 0.01$, 1, and 100.

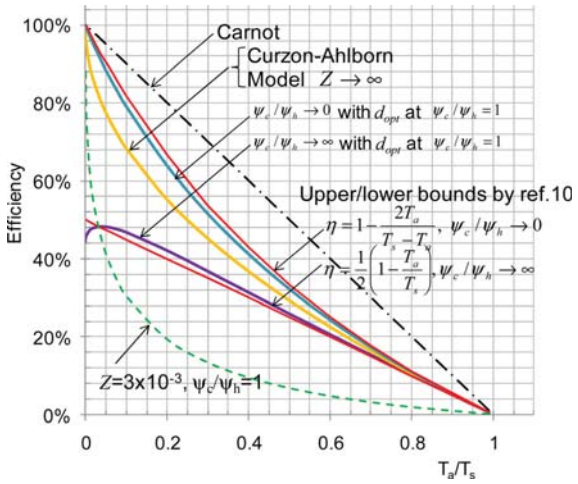

FIG. 3. (Color online) Efficiency at maximum power output as a function of T_a/T_s, the model at infinite Z, perfectly matches Curzon-Ahlborn at any ψ_c/ψ_h. The limits of the thermodynamic cyclic engines (Ref. 11) and the curves for $Z = 3 \times 10^{-3}$ with $\psi_c/\psi_h = 1$ are also shown.

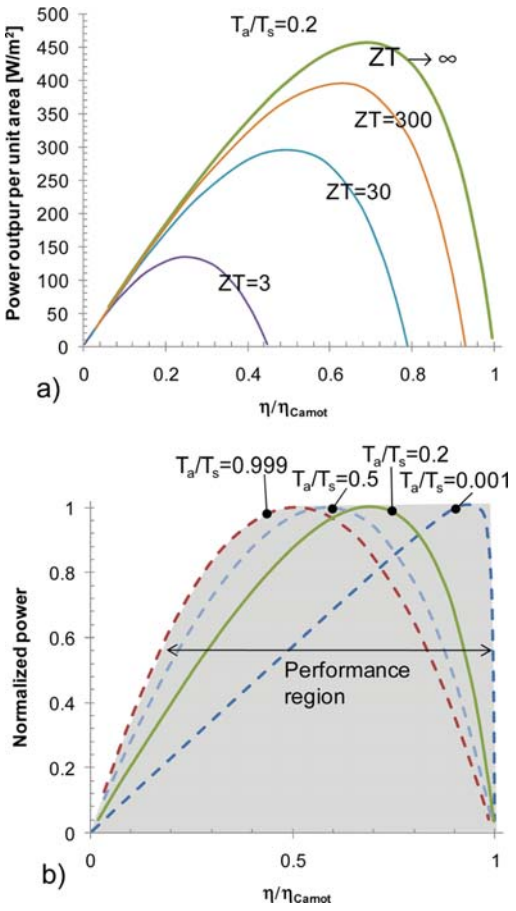

FIG. 4. (Color online) Output power as a function of efficiency (a) varying ZT for $T_a/T_s = 0.2$ and (b) varying T_a/T_s with power normalized with respect to the peak power value of the individual curves. $T_a = 300$ K fixed, $\Sigma\psi = 1.0$, $\psi_c = \psi_h$, and only thermal conductivity is modified for various ZT.

$1 - T_a/T_s$, where leg length d becomes extremely large and then power output diminishes. Figure 4(b) is the normalized power output with different T_a/T_s ratios. The curves represent the case where ZT is infinity. There is a region of very low efficiency in Fig. 4(b) where the power output does not exist. This region is identified outside of the hatched area in the figure.

Carnot limit is always reached when the output power is zero. In the case when ambient reservoir temperature is much smaller than the heat source temperature (Fig. 4(b), $T_a/T_s = 0.001$), we see that maximum output power can be reached at an efficiency very close to Carnot limit. The temperature gradient is so large that one can get lots of power with very high efficiency. For the opposite extreme case, when T_s is close to T_a, the maximum power is observed when the efficiency equals half of the Carnot efficiency.

It is interesting to compare the results with the quantum dot (QD) thermoelectric engine investigated by Nakpathomkun *et al.*[13] In their study, delta function differential conductivity (transport function) can produce an "ideal" thermoelectric material with Carnot efficiency. Nakpathomkun *et al*. correlate the transfer function of QD with the ZT of bulk materials. For comparison, Figs. 5(a) and 5(b) show the power output of our model with corresponding ZT values to QD engines as a function of the normalized efficiency to that of Carnot η/η_C. The curves are obtained by modifying the load resistance (m). These curves are similar to the QD ones in lower power output ranges and for efficiency at maximum output power. Like QD, the maximum efficiency is independent of temperature when ZT is fixed. However, the maximum efficiency is lower than QD. This may happen because the bulk materials have finite thermal conductivity, and our calculation is always optimizing the system with finite leg length to match external thermal impedances. Thermal resistances with reservoirs were not explicitly included in the case of quantum dot heat engines. In the classical thermoelectric systems, there is always a finite thermal resistance between reservoirs (T_s and T_a) and the hot (T_h) and cold (T_c) junctions of the thermoelectric element. Thus, T_h and T_c are different from T_s and T_a. On the other hand, in the quantum dot case, only two temperatures, T_s and T_a, enter in the calculations. Coupling with reservoirs and discrete energy level broadening limit the charge flow (electrical resistance) as well as electronic heat flow through the quantum dot. However, there is no explicit thermal resistance between the hot side of the quantum dot and the hot reservoir and the same for the cold side. It seems that inherently ideal "thermal" contacts are assumed. If one adds non-ideal thermal contacts, then some of the results on bulk thermoelectric system described in this paper could be directly compared with the quantum dots.

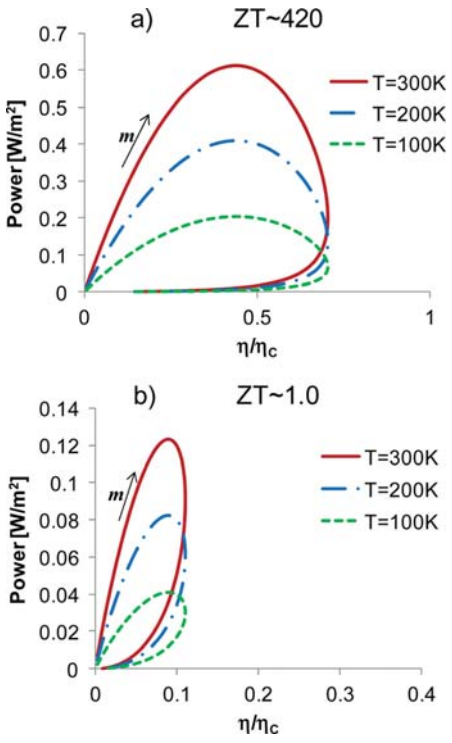

FIG. 5. (Color online) Output power as a function of efficiency η/η_C. (a) ZT $\sim$ 420 equivalent to $\Gamma = 0.01$ kT and (b) ZT $\sim$ 1.0 equivalent to $\Gamma = 2.25$ kT of QD (Ref. 13). $\Delta T/T_a = 0.1$ and $T_a = 100, 200, 300$ K, $\psi_c = \psi_h$.

Another fundamental difference between bulk thermoelectric material and single quantum dot material is that coupling with reservoirs broadens the quantum dot energy level, and this modifies the "effective" Z of the quantum dot material. Electrical conductivity, Seebeck coefficient, and electronic thermal conductivity depend on the width of the energy level. Because the "effective" Z is not an inherent property of the dot, one cannot have Curzon-Ahlborn limit (finite output power) with infinitely large Z (requiring delta function density-of-states). However, in the case of bulk material, Z is given and thermal and electrical contacts with reservoirs do not change the inherent material properties. Given any thermal contact resistances with reservoirs, one can optimize the thermoelectric leg length and the load resistance to get either the highest output power or the highest energy conversion efficiency.

V. SUMMARY

We have modeled and analyzed a generic thermoelectric power generation system that contains asymmetric thermal contacts with hot and cold reservoirs. The maximum power output is found when the load electrical resistance divided by the thermoelectric element resistance is given by sqrt$(1 + ZT)$ and when the temperature difference across the leg is approximately half of the total temperature span. For the symmetric contacts with the reservoirs, this temperature ratio is exactly half and the thermal resistance ratio is equal to the electrical resistance ratio.

System energy conversion efficiency at maximum power output always follows the Curzon-Ahlborn limit when the figure of merit Z is very large. An infinitely large Z makes the thermoelectric leg exactly the same as the reversible heat engine when the temperatures for both hot side and cold side are ideally given. However, due to the co-optimization of both electrical and thermal networks and the fact that the thermoelectric leg is always in contact with both hot and cold reservoirs, the efficiency at the maximum power output shows different behavior compared to cyclic thermodynamic engines for asymmetric thermal contacts with reservoirs.

Interestingly, the thermoelectric efficiency limit at maximum output power for the case of asymmetric thermal contacts with hot and cold reservoirs approaches the limits obtained by Esposito *et al.*[11] when the thermoelectric leg thickness is fixed to the optimum value used in the symmetric case (see Fig. 2). Further optimization of the leg thickness yields the Curzon-Ahlborn result. One should emphasize that the bulk analysis in this paper is valid for "any" Z value. Figure 3 focuses on the infinite Z. However, the rest of the analysis is done with Z (or ZT) as a variable. The bulk thermoelectric model was also compared with ideal quantum dot heat engines, which are based on delta function differential conductivity and displayed similarities and also differences. This inconsistency may come from the limitation of the bulk systems given by finite thermal resistances with reservoirs, which is not included in the standard treatment of the quantum systems.

ACKNOWLEDGMENTS

This work was supported by the Center for Energy Efficient Materials, funded by the Office of Basic Energy Sciences of the U.S. Department of Energy. A.S. acknowledges stimulating discussions with Prof. S. Datta.

[1]F. D. Rosi, E. F. Hockings, and N. E. Lindenblad, RCA Rev. **22**, 82 (1961).
[2]D. Vashaee and A. Shakouri, J. Appl. Phys. **101**(5), 053719 (2007).
[3]M. S. Dresselhaus, G. Chen, M. Y. Tang, L. Ronggui, H. Lee, D. Wang, Z. Ren, J. Fleurial, and P. Gogna, Adv. Mater. **19**(8), 1043 (2007).
[4]K. Yazawa and A. Shakouri, in *Proceedings of the ASME 2010 International Mechanical Engineering Congress and Exposition*, Vancouver, British Columbia, 12–18 November 2010.
[5]P. M. Mayer and R. J. Ram, Nanoscale Microscale Thermophys. Eng. **10**, 143 (2006).
[6]J. W. Stevens, Energy Convers. Manage. **42**, 709 (2001).
[7]G. J. Snyder, *Energy Harvesting Technologies*, edited by S. Priya, D. J. Inman, Springer, New York (2009), pp. 330–331.
[8]M. Esposito, K. Lindenberg, and C. Van Den Broeck, EPL **85**, 60010 (2009).
[9]M. Freunek, M. Muller, T. Ungan, W. Walker, and L. M. Reindl, J. Electron. Mater. **38**(7), 1214 (2009).
[10]F. Curzon and B. Ahlborn, Am. J. Phys. **43**, 22 (1975).
[11]M. Esposito, R. Kawai, K. Lindenberg, and C. Van Den Broeck, Phys. Rev. Lett. **105**, 150603 (2010).
[12]K. Yazawa and A. Shakouri, Environ. Sci. Technol. **45**(17), 7548 (2011).
[13]N. Nakpathomkun, H. Q. Xu, and H. Linke, Phys. Rev. B **82**, 235428 (2010).